



Ecole doctorale n°572 Ondes et Matière (EDOM)
Spécialité de doctorat: Physique des Plasmas

Full Name

Composition du Jury :

[illegible]



Numerical study of electron transport in Hall Thrusters

Thèse de doctorat de l'Institut Polytechnique de Paris
préparée à École polytechnique

École doctorale n°626 Institut Polytechnique de Paris (IPP)
Spécialité de doctorat : Physique des Plasmas

Thèse présentée et soutenue à Palaiseau, le 30/09/2020, par

THOMAS CHAROY

Composition du Jury :

Jean-Pierre Boeuf Directeur de recherche, CNRS, LAPLACE (Université Paul Sabatier)	Président
Eduardo Ahedo Professeur, Université Carlos III, Madrid	Rapporteur
Francesco Taccogna Chercheur, IMIP/CNR	Rapporteur
Nicolas Plihon Chargé de recherche, CNRS, Laboratoire de Physique (ENS de Lyon)	Examineur
Andrei Smolyakov Professeur, University of Saskatchewan	Examineur
Anne Bourdon Directeur de Recherche, CNRS, LPP, École polytechnique	Directrice de thèse
Pascal Chabert Directeur de Recherche, CNRS, LPP, École polytechnique	Co-directeur de thèse
Olivier Duchemin Ingénieur, Safran Aircraft Engines	Invité

Acknowledgment

Lorem ipsum dolor sit amet, consectetur adipiscing elit. Ut purus elit, vestibulum ut, placerat ac, adipiscing vitae, felis. Curabitur dictum gravida mauris. Nam arcu libero, nonummy eget, consectetur id, vulputate a, magna. Donec vehicula augue eu neque. Pellentesque habitant morbi tristique senectus et netus et malesuada fames ac turpis egestas. Mauris ut leo. Cras viverra metus rhoncus sem. Nulla et lectus vestibulum urna fringilla ultrices. Phasellus eu tellus sit amet tortor gravida placerat. Integer sapien est, iaculis in, pretium quis, viverra ac, nunc. Praesent eget sem vel leo ultrices bibendum. Aenean faucibus. Morbi dolor nulla, malesuada eu, pulvinar at, mollis ac, nulla. Curabitur auctor semper nulla. Donec varius orci eget risus. Duis nibh mi, congue eu, accumsan eleifend, sagittis quis, diam. Duis eget orci sit amet orci dignissim rutrum.

Nam dui ligula, fringilla a, euismod sodales, sollicitudin vel, wisi. Morbi auctor lorem non justo. Nam lacus libero, pretium at, lobortis vitae, ultricies et, tellus. Donec aliquet, tortor sed accumsan bibendum, erat ligula aliquet magna, vitae ornare odio metus a mi. Morbi ac orci et nisl hendrerit mollis. Suspendisse ut massa. Cras nec ante. Pellentesque a nulla. Cum sociis natoque penatibus et magnis dis parturient montes, nascetur ridiculus mus. Aliquam tincidunt urna. Nulla ullamcorper vestibulum turpis. Pellentesque cursus luctus mauris.

Résumé

Lorem ipsum dolor sit amet, consectetur adipiscing elit. Ut purus elit, vestibulum ut, placerat ac, adipiscing vitae, felis. Curabitur dictum gravida mauris. Nam arcu libero, nonummy eget, consectetur id, vulputate a, magna. Donec vehicula augue eu neque. Pellentesque habitant morbi tristique senectus et netus et malesuada fames ac turpis egestas. Mauris ut leo. Cras viverra metus rhoncus sem. Nulla et lectus vestibulum urna fringilla ultrices. Phasellus eu tellus sit amet tortor gravida placerat. Integer sapien est, iaculis in, pretium quis, viverra ac, nunc. Praesent eget sem vel leo ultrices bibendum. Aenean faucibus. Morbi dolor nulla, malesuada eu, pulvinar at, mollis ac, nulla. Curabitur auctor semper nulla. Donec varius orci eget risus. Duis nibh mi, congue eu, accumsan eleifend, sagittis quis, diam. Duis eget orci sit amet orci dignissim rutrum.

Nam dui ligula, fringilla a, euismod sodales, sollicitudin vel, wisi. Morbi auctor lorem non justo. Nam lacus libero, pretium at, lobortis vitae, ultricies et, tellus. Donec aliquet, tortor sed accumsan bibendum, erat ligula aliquet magna, vitae ornare odio metus a mi. Morbi ac orci et nisl hendrerit mollis. Suspendisse ut massa. Cras nec ante. Pellentesque a nulla. Cum sociis natoque penatibus et magnis dis parturient montes, nascetur ridiculus mus. Aliquam tincidunt urna. Nulla ullamcorper vestibulum turpis. Pellentesque cursus luctus mauris.

Nulla malesuada porttitor diam. Donec felis erat, congue non, volutpat at, tincidunt tristique, libero. Vivamus viverra fermentum felis. Donec nonummy pellentesque ante. Phasellus adipiscing semper elit. Proin fermentum massa ac quam. Sed diam turpis, molestie vitae, placerat a, molestie nec, leo. Maecenas lacinia. Nam ipsum ligula, eleifend at, accumsan nec, suscipit a, ipsum. Morbi blandit ligula feugiat magna. Nunc eleifend consequat lorem. Sed lacinia nulla vitae enim. Pellentesque tincidunt purus vel magna. Integer non enim. Praesent euismod nunc eu purus. Donec bibendum quam in tellus. Nullam cursus pulvinar lectus. Donec et mi. Nam vulputate metus eu enim. Vestibulum pellentesque felis eu massa.

Quisque ullamcorper placerat ipsum. Cras nibh. Morbi vel justo vitae lacus tincidunt ultrices. Lorem ipsum dolor sit amet, consectetur adipiscing elit. In hac habitasse platea dictumst. Integer tempus convallis augue. Etiam facilisis. Nunc elementum fermentum wisi. Aenean placerat. Ut imperdiet, enim sed gravida

sollicitudin, felis odio placerat quam, ac pulvinar elit purus eget enim. Nunc vitae tortor. Proin tempus nibh sit amet nisl. Vivamus quis tortor vitae risus porta vehicula.

Fusce mauris. Vestibulum luctus nibh at lectus. Sed bibendum, nulla a faucibus semper, leo velit ultricies tellus, ac venenatis arcu wisi vel nisl. Vestibulum diam. Aliquam pellentesque, augue quis sagittis posuere, turpis lacus congue quam, in hendrerit risus eros eget felis. Maecenas eget erat in sapien mattis porttitor. Vestibulum porttitor. Nulla facilisi. Sed a turpis eu lacus commodo facilisis. Morbi fringilla, wisi in dignissim interdum, justo lectus sagittis dui, et vehicula libero dui cursus dui. Mauris tempor ligula sed lacus. Duis cursus enim ut augue. Cras ac magna. Cras nulla. Nulla egestas. Curabitur a leo. Quisque egestas wisi eget nunc. Nam feugiat lacus vel est. Curabitur consectetur.

Suspendisse vel felis. Ut lorem lorem, interdum eu, tincidunt sit amet, laoreet vitae, arcu. Aenean faucibus pede eu ante. Praesent enim elit, rutrum at, molestie non, nonummy vel, nisl. Ut lectus eros, malesuada sit amet, fermentum eu, sodales cursus, magna. Donec eu purus. Quisque vehicula, urna sed ultricies auctor, pede lorem egestas dui, et convallis elit erat sed nulla. Donec luctus. Curabitur et nunc. Aliquam dolor odio, commodo pretium, ultricies non, pharetra in, velit. Integer arcu est, nonummy in, fermentum faucibus, egestas vel, odio.

Sed commodo posuere pede. Mauris ut est. Ut quis purus. Sed ac odio. Sed vehicula hendrerit sem. Duis non odio. Morbi ut dui. Sed accumsan risus eget odio. In hac habitasse platea dictumst. Pellentesque non elit. Fusce sed justo eu urna porta tincidunt. Mauris felis odio, sollicitudin sed, volutpat a, ornare ac, erat. Morbi quis dolor. Donec pellentesque, erat ac sagittis semper, nunc dui lobortis purus, quis congue purus metus ultricies tellus. Proin et quam. Class aptent taciti sociosqu ad litora torquent per conubia nostra, per inceptos hymenaeos. Praesent sapien turpis, fermentum vel, eleifend faucibus, vehicula eu, lacus.

Summary

Lorem ipsum dolor sit amet, consectetur adipiscing elit. Ut purus elit, vestibulum ut, placerat ac, adipiscing vitae, felis. Curabitur dictum gravida mauris. Nam arcu libero, nonummy eget, consectetur id, vulputate a, magna. Donec vehicula augue eu neque. Pellentesque habitant morbi tristique senectus et netus et malesuada fames ac turpis egestas. Mauris ut leo. Cras viverra metus rhoncus sem. Nulla et lectus vestibulum urna fringilla ultrices. Phasellus eu tellus sit amet tortor gravida placerat. Integer sapien est, iaculis in, pretium quis, viverra ac, nunc. Praesent eget sem vel leo ultrices bibendum. Aenean faucibus. Morbi dolor nulla, malesuada eu, pulvinar at, mollis ac, nulla. Curabitur auctor semper nulla. Donec varius orci eget risus. Duis nibh mi, congue eu, accumsan eleifend, sagittis quis, diam. Duis eget orci sit amet orci dignissim rutrum.

Nam dui ligula, fringilla a, euismod sodales, sollicitudin vel, wisi. Morbi auctor lorem non justo. Nam lacus libero, pretium at, lobortis vitae, ultricies et, tellus. Donec aliquet, tortor sed accumsan bibendum, erat ligula aliquet magna, vitae ornare odio metus a mi. Morbi ac orci et nisl hendrerit mollis. Suspendisse ut massa. Cras nec ante. Pellentesque a nulla. Cum sociis natoque penatibus et magnis dis parturient montes, nascetur ridiculus mus. Aliquam tincidunt urna. Nulla ullamcorper vestibulum turpis. Pellentesque cursus luctus mauris.

Nulla malesuada porttitor diam. Donec felis erat, congue non, volutpat at, tincidunt tristique, libero. Vivamus viverra fermentum felis. Donec nonummy pellentesque ante. Phasellus adipiscing semper elit. Proin fermentum massa ac quam. Sed diam turpis, molestie vitae, placerat a, molestie nec, leo. Maecenas lacinia. Nam ipsum ligula, eleifend at, accumsan nec, suscipit a, ipsum. Morbi blandit ligula feugiat magna. Nunc eleifend consequat lorem. Sed lacinia nulla vitae enim. Pellentesque tincidunt purus vel magna. Integer non enim. Praesent euismod nunc eu purus. Donec bibendum quam in tellus. Nullam cursus pulvinar lectus. Donec et mi. Nam vulputate metus eu enim. Vestibulum pellentesque felis eu massa.

Quisque ullamcorper placerat ipsum. Cras nibh. Morbi vel justo vitae lacus tincidunt ultrices. Lorem ipsum dolor sit amet, consectetur adipiscing elit. In hac habitasse platea dictumst. Integer tempus convallis augue. Etiam facilisis. Nunc elementum fermentum wisi. Aenean placerat. Ut imperdiet, enim sed gravida

sollicitudin, felis odio placerat quam, ac pulvinar elit purus eget enim. Nunc vitae tortor. Proin tempus nibh sit amet nisl. Vivamus quis tortor vitae risus porta vehicula.

Fusce mauris. Vestibulum luctus nibh at lectus. Sed bibendum, nulla a faucibus semper, leo velit ultricies tellus, ac venenatis arcu wisi vel nisl. Vestibulum diam. Aliquam pellentesque, augue quis sagittis posuere, turpis lacus congue quam, in hendrerit risus eros eget felis. Maecenas eget erat in sapien mattis porttitor. Vestibulum porttitor. Nulla facilisi. Sed a turpis eu lacus commodo facilisis. Morbi fringilla, wisi in dignissim interdum, justo lectus sagittis dui, et vehicula libero dui cursus dui. Mauris tempor ligula sed lacus. Duis cursus enim ut augue. Cras ac magna. Cras nulla. Nulla egestas. Curabitur a leo. Quisque egestas wisi eget nunc. Nam feugiat lacus vel est. Curabitur consectetur.

Table of Content

Table of Content	vii
List of notes	ix
List of Figures	xi
List of Tables	xiii
Acronyms	xv
Nomenclature and List of Symbols	xvii
1 Concepts and preliminaries	1
1.1 Propulsion system for spacecrafts	1
1.1.1 The rocket equation	2
1.1.2 Electric propulsion systems	2
1.1.3 Electric propulsion environment in France	3
1.2 Electric propulsion challenges	5
2 Particle-In-Cell simulations of HETs	7
2.1 Elements of the 2D PIC-MCC simulations	8
2.1.1 The PIC simulations	8
2.1.2 The Monte Carlo collisions	8
3 Study of dielectric impact on mobility	11
3.1 Presentation of the study	12
3.2 The base case	14
3.2.1 Initial phase of the simulation : $t < 2\mu\text{s}$	14
3.2.2 Saturated quasi steady-state : $t \geq 2\mu\text{s}$	15
3.2.3 Enhanced electron transport	16

4 Conclusion 21

4.1 Summary of the thesis 21



4.1.1 Growth and saturation of the azimuthal instability 22

4.1.2 Impact of the wall characteristics on the plasma-wall inter-
action 22

A Scalability tests 23

Bibliography 27

Todo list

	more informations could be added here!	12
	unsure here	12

List of Figures

1.1	The T6 ion thruster will help send BepiColombo to Mercury. The neutralizing cathode is in the upper left quadrant of the thruster. (Credit : QinetiQ)	3
1.2	A 13 kilowatt HET prototype on a testing bench in a vacuum chamber (Credit : NASA).	4
2.1	Cross section values used in the Monte Carlo procedure [1, 2].	9
3.1	Temporal evolution of the electron mean kinetic energy decomposed over the three directions. Only the beginning of the simulation is shown.	14
3.2	Temporal evolution of the radial profile of the (a) electron density and (b) the plasma potential averaged azimuthally.	15
3.3	Temporal evolution of the electron mean kinetic energy decomposed over the three directions, similar to Fig. 3.1 but for a longer period. We still see the difference between \mathcal{E}_{ez} and $\mathcal{E}_{e\theta}$ due to the $E \times B$ drift, and the colder radial energy.	16
3.4	Radial profile of the ion and electron densities at steady-state, averaged azimuthally and in time over the 5 last microseconds.	17
3.5	Temporal evolution of the electron axial mobility computed in the PIC simulation.	18
3.6	Azimuthal instability : temporal evolution of the azimuthal electric field at the center of the simulations, and its frequency spectrum computed by FFT. The frequency for which the amplitude is maximum is highlighted.	19

List of Tables

1.1	Members of the PPS® series developed by Safran Aircraft Engines [3, 4, 5]. The nominal operating condition of the PPS®X00 is not fixed yet.	4
2.1	Reactions for xenon used in the PIC simulations	9
3.1	Standard operating and numerical parameters used in the 2D PIC simulations of an HET. The simulation results are given as representative values.	13
3.2	Characteristics measured in the simulation at $t = 27 \mu\text{s}$	18
A.1	Operating and numerical parameters used in the strong scalability large test-case.	24
A.2	Modified parameter for the strong-scalability small test-case. The other parameters are given in Table A.1.	25
A.3	Performances of the large test-case (parameters of Table A.1) when using 96 CPUs, average over 1000 time steps.	25

Acronyms

1D	1 dimension
2D	2 dimensions
3D	3 dimensions
3V	3 dimension for the velocity
BC	Boundary Conditions
BN	Boron Nitride
BNSiO₂	Boron Nitride-Silicon Dioxide. A ceramic composed of a mix of Boron Nitride and Silicon Dioxide.
CNES	Centre National d'Etude Spatial. The French space agency
DFT	Discrete Fourier Transform
DK	Direct Kinetic
DR	Dispersion Relation . Relation between the wave number and complex frequency for waves in plasmas.
ECDI	Electron Cyclotron Drift Instability. Another name of the EDI present in HET.
EDI	$E \times B$ Electron Drift Instability. Another name of the ECDI present in HET.
EEDF	Electron Energy Distribution Function
EEPF	Electron Energy Probability Function
EP	Electric Propulsion. Propulsion engines using the electric energy, instead of the chemical energy.
EVDF	Electron Velocity Distribution Function
FT	Fourier Transform
FFT	Fast Fourier Transform
GEO	GEostationary Orbit Corresponds to the Orbit that follows the Earth rotation. Used mainly for telecommunication (Like the French Canal (former Canalsat)), it lies at 36000km from the Earth.

HET	Hall Effect Thruster
IAW	Ion Acoustic Wave
Kr	Krypton
LEO	Low Earth Orbit The LEO corresponds to orbits of altitude lower than 2000 km. Mostly used for Earth observation, and the ISS.
LHS	Left Hand Side
LPP	Laboratoire de Physique des Plasmas A laboratory from Ecole polytechnique, Palaiseau, France .
MCC	Monte Carlo Collision
ML	Laboratory Model
MTSI	Modified Two Stream Instability
NWC	Near-Wall Conductivity. Increased cross-field transport due to electron-wall collision and electron emissions from the wall.
PIC	Particle In Cell
RF	Radio Frequency
RMS	Root Mean Square
RSO	Relaxation Sheath Oscillation Oscillations between the SCL and the usual sheath regimes
SCL	Space Charge Limited
SEE	Secondary Electron Emission. Electron emission from a wall due to an energetic impact of a primary electron.
Xe	xenon

Nomenclature and List of Symbols

In this work we use the SI system of units, except for a few units specific to the plasma community that are describe below. The notations in general follow common usage. The vectors are noted in bold, as \mathbf{v} , \mathbf{E} , etc. Complex quantities are not distinguished from real ones.

The next list describes several symbols that will be later used within the body of the document.

Physics Constants

e	Elementary charge	$1.602176634 \times 10^{-19} \text{ C}$
g_0	Standard acceleration due to gravity	9.80665 m/s^2
K_B	Boltzmann constant	$1.380649 \times 10^{-23} \text{ J/K}$
eV	Unit of energy, corresponds to the kinetic energy of one electron accelerated by an electric potential difference of one volt. It is usually used in plasma physics as a unit of temperature via the Boltzmann constant.	$1 \text{ eV} \simeq 1.602 \times 10^{-19} \text{ J}$
Gauss	Unit of magnetic flux density in cgs (centimeter-gram-second units)	$1 \text{ G} = 1 \times 10^{-4} \text{ T}$
Torr	Equivalent to one millimeter of mercury,	$1 \text{ Torr} = 133.32 \text{ Pa}$

Quantities

Δv	Measure of impulse needed for a space manoeuvre
\mathcal{E}_e	Electron total kinetic energy, imposed of the thermal (or internal) energy and the kinetic energy of the mean velocity.
I_{sp}	Specific impulse, related to the exhaust velocity of a propellant
M	Mass of a spacecraft
T	Thrust
t	Time
u_e, u_i	Electron and ion mean velocities

Chapitre 1

Concepts and preliminaries

The Earth is the cradle of humanity, but mankind cannot stay in the cradle forever.

Konstantin Tsiolkovsky, *pioneer of the astronautic theory*

Contents

1.1	Propulsion system for spacecrafts	1
1.1.1	The rocket equation	2
1.1.2	Electric propulsion systems	2
1.1.3	Electric propulsion environment in France	3
1.2	Electric propulsion challenges	5

1.1 Propulsion system for spacecrafts

In order to move in space, satellites, scientific probes, and spacecrafts in general rely on a propulsion system. The cost to go from one location to another can be expressed as Δv , a measure of impulse needed to maneuver. ?? illustrates the Δv required to evolve in the solar system. We can see that reaching Low Earth Orbit (LEO) needs a Δv of 9400 m/s while the GEostationary Orbit (GEO) is 3910 m/s further. Landing on the Moon from the Earth ground requires a total of 15 km/s, while landing on Neptune requires $\Delta v = 43.7$ km/s. For a spacecraft of instantaneous mass $M(t)$, with a propulsion system generating a thrust $T(t)$, the Δv between t_1 and t_2 is

$$\Delta v = \int_{t_1}^{t_2} \frac{|T(t)|}{M(t)} dt. \tag{1.1}$$

1.1.1 The rocket equation

The thrust T generated by ejecting mass at high velocity is

$$T = v_{\text{ex}} \dot{M} \quad (1.2)$$

with v_{ex} the exhaust velocity of the propellant, and \dot{M} the propellant mass flow rate through the thruster. Hence,

$$\Delta v = \int_{t_1}^{t_2} v_{\text{ex}} \frac{|\dot{M}|}{M(t)} dt = v_{\text{ex}} \ln \left(\frac{M_0}{M_1} \right) \quad (1.3)$$

with $M_0 = M(t_0)$ and $M_1 = M(t_1)$, and supposing that v_{ex} is constant. We see from Eq. (1.3) that for a spacecraft of dry mass M_1 to have a given Δv , the exhaust velocity is directly linked to the initial *wet* mass $M_0 = M_1 + M_{\text{prop}}$, with M_{prop} the propellant mass. Equation (1.3) is known as the rocket equation, or Tsiolkovsky's equation. Usually, instead of the exhaust velocity v_{ex} , the specific impulse $I_{\text{sp}} = g_0 v_{\text{ex}}$, with g_0 the standard gravity, is used.

1.1.2 Electric propulsion systems

Electric Propulsion (EP) systems mostly rely on plasmas [6, 7]. They have been successfully used since the 1960s by governments, but their complexity, the limited electric power available, and the inherent risk aversion of the space industry kept the EP technologies hidden from the commercial applications [8]. The breakthrough came in the '90s when the former Soviet Union's companies licensed the technology to Western propulsion companies. However, many commercial satellite manufacturers were skeptical, until the first decade of the 21st century, which brought strong evidence of the competitiveness of EP. The landmark of commercial use of EP is the selling of four all-electric satellites for GEO by Boeing in 2012, the first two of which were launched in March 2015.

The two leading EP technologies used are

- the Hall Effect Thruster (HET), also known as Stationary Plasma Thruster (SPT) in Russia
- the Gridded Ion Thruster (GIT), usually referred simply as Ion Thruster

The Gridded Ion Thruster is a plasma chamber closed at one end by two or more grids. The plasma source can be an emitting cathode, generating energetic electrons that ionize the propellant (usually Xenon), or a Radio Frequency (RF) source. The potential difference between the grids accelerates the ions. Another cathode is used to neutralize the ion beam. Compared to HETs, it produces an ion beam with less divergence and a higher I_{sp} of the order of 3000 to 4000 s. Figure 1.1 shows a picture of the ion thruster used for the BepiColombo mission toward Mercury. We see the neutralizing cathode, the accelerating grid, and the ion beam.

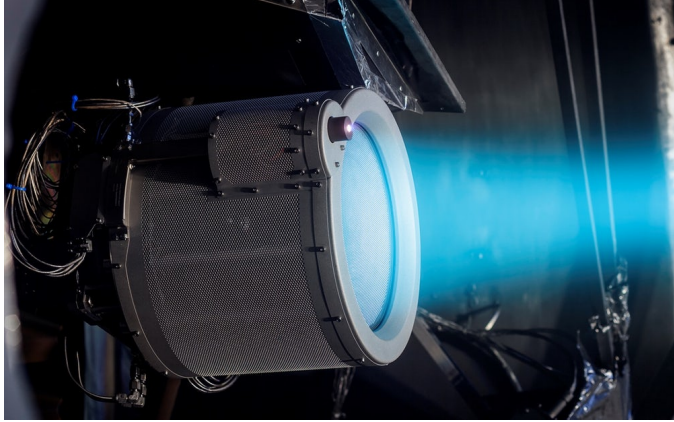


FIGURE 1.1 – The T6 ion thruster will help send BepiColombo to Mercury. The neutralizing cathode is in the upper left quadrant of the thruster. (Credit: QinetiQ)

Hall Effect thrusters use a magnetic barrier to both increase the ionization of the propellant and create the accelerating electric field. A detailed description of the HET is presented in the next section. One cathode is used to start the discharge and neutralize the ion beam. Compared to GITs, HETs need less power, hence reaching better thrust per power ratio and a smaller (therefore lighter) Power Processing Unit. Recently, the first satellites of two mega-constellations (OneWeb, 648 satellites planned, from which six were launched on February, 26th 2019, and Starlink, 12 000 satellites planned, from which 62 were launched on May, 23rd 2019) were sent to Low Earth orbit, both using HETs.

Their typical I_{sp} is of the order of 1500 s. Figure 1.2 shows a high power prototype firing. We see the emitting cathode, in this design at the center, and the ion beam.

1.1.3 Electric propulsion environment in France

France is a leader country in the aerospace industry in both Europe and the world, with companies such as Airbus, Thales, Safran, and ArianeGroup (joint-venture of Safran and Airbus). As a consequence, the French ecosystem of electric propulsion is vibrant. The main thrusters produced in France are the PPS series by Safran, with the PPS®1350 (version G at 1.5 kW nominal power, and the version E at 2.7 kW), and the PPS®5000, a high power HET at 5 kW, the first models of which have been delivered to Boeing in May 2019. A low-power version (between 500W and 1kW) of the PPS® is currently developed[5]. A list for the PPS® series elements and their respective characteristics can be seen in Table 1.1.

Several initiatives concerning the small-sat sector are also undertaken, such as the start-ups Exotrail (micro HET) and Thrust Me (radio frequency Ion Thruster), or the Electron Cyclotron Resonance Thruster at ONERA. Since 1996, numerous

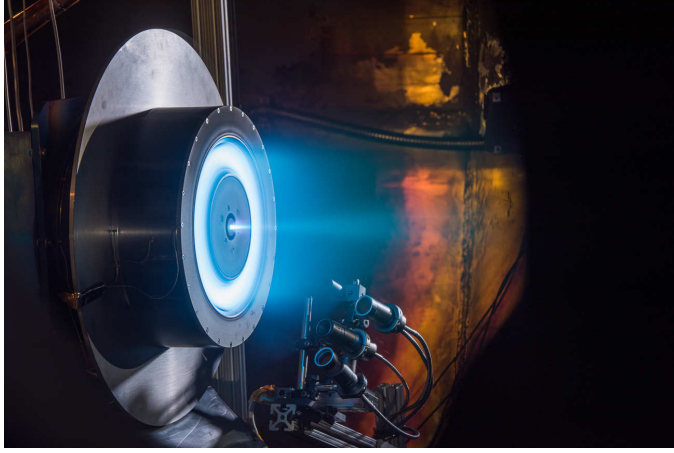


FIGURE 1.2 – A 13 kilowatt HET prototype on a testing bench in a vacuum chamber (Credit: NASA).

TABLE 1.1 – Members of the PPS® series developed by Safran Aircraft Engines [3, 4, 5]. The nominal operating condition of the PPS®X00 is not fixed yet.

Name	Power	Thrust	I_{sp}
PPS®1350-G	1.5 kW	89 mN	1650 s
PPS®1350-E	2.7 kW	140 mN	1800 s
PPS®5000	3 – 5 kW	150 – 300 mN	1850 – 1700 s
PPS®X00	~ 650W	~40 mN	~ 1450 s

research projects have been carried out in France on HET with the Centre National d’Etude Spatial (CNES), SAFRAN and several research laboratories : ICARE, LAPLACE, CPHT, LPP, etc. [3]. These numerous actors, combined with the support of the French and European space agencies, compose a stimulating environment that contributes both to the most mature technologies and the promising EP concepts that could disrupt the propulsion sector.

1.2 Electric propulsion challenges

Several challenges are currently tackled in the EP industry. The most prominent are listed by Samukawa et al. [9]:

1. Performance improvement: efficiency, lifetime, and cost-effectiveness. Lifetime is an important issue and is limited by electrode or wall erosion. The lifetime of an electric thruster must be larger than 10 000 h of (reliable) operation.
2. Design of more versatile thrusters, i.e. able to operate at different combinations of thrust and propellant velocity.
3. Extension of the domain of operation to lower power (μN to 10 mN thrust range) for microsatellites or accurate attitude control.
4. Extension to higher power for orbit raising of telecommunication satellites (several tens of kW) and interplanetary missions (100 kW and more).
5. Extension of EP to low-altitude spacecraft: there is an increasing interest in civilian and military satellites flying at altitudes around 100 km where the drag is significant and must be continuously compensated.

HET technology has the potential to answer many of these challenges. For instance, the lifetime issue can be addressed with wall-less and magnetically shielded configurations. Versatility is tackled with dual-mode HET configuration [3], low power thruster is attained with μ -thrusters [10], and so forth. However, the development of HETs is slow and expensive. A better physical understanding of the processes governing HETs is needed in order to reduce the cost and development times. This is the objective of the current collaboration between Safran Aircraft Engines and Laboratoire de Physique des Plasmas (LPP).

Chapitre 2

Particle-In-Cell simulations of HETs

Lorem ipsum dolor sit amet, consectetur adipiscing elit. Ut purus elit, vestibulum ut, placerat ac, adipiscing vitae, felis. Curabitur dictum gravida mauris. Nam arcu libero, nonummy eget, consectetur id, vulputate a, magna. Donec vehicula augue eu neque. Pellentesque habitant morbi tristique senectus et netus et malesuada fames ac turpis egestas. Mauris ut leo. Cras viverra metus rhoncus sem. Nulla et lectus vestibulum urna fringilla ultrices. Phasellus eu tellus sit amet tortor gravida placerat. Integer sapien est, iaculis in, pretium quis, viverra ac, nunc. Praesent eget sem vel leo ultrices bibendum. Aenean faucibus. Morbi dolor nulla, malesuada eu, pulvinar at, mollis ac, nulla. Curabitur auctor semper nulla. Donec varius orci eget risus. Duis nibh mi, congue eu, accumsan eleifend, sagittis quis, diam. Duis eget orci sit amet orci dignissim rutrum.

Nam dui ligula, fringilla a, euismod sodales, sollicitudin vel, wisi. Morbi auctor lorem non justo. Nam lacus libero, pretium at, lobortis vitae, ultricies et, tellus. Donec aliquet, tortor sed accumsan bibendum, erat ligula aliquet magna, vitae ornare odio metus a mi. Morbi ac orci et nisl hendrerit mollis. Suspendisse ut massa. Cras nec ante. Pellentesque a nulla. Cum sociis natoque penatibus et magnis dis parturient montes, nascetur ridiculus mus. Aliquam tincidunt urna. Nulla ullamcorper vestibulum turpis. Pellentesque cursus luctus mauris.

Contents	
2.1	Elements of the 2D PIC-MCC simulations 8
2.1.1	The PIC simulations 8
2.1.2	The Monte Carlo collisions 8

2.1 Elements of the 2D PIC-MCC simulations

2.1.1 The PIC simulations

The Particle In Cell (PIC) simulation models particles moving freely on a grid. The grid is used to compute the electric field, in the electrostatic approximation by solving the Poisson equation

$$\Delta\phi = -\frac{\rho}{\epsilon_0} \quad (2.1)$$

where ϕ is the electric potential, ρ is the charge density, and ϵ_0 the vacuum permittivity. If the electrostatic approximation is not correct, one needs to solve the Maxwell equations.

The particles move following the Lorentz forces

$$m\frac{\partial\mathbf{v}}{\partial t} = q\mathbf{E} + q\mathbf{v} \times \mathbf{B} \quad (2.2)$$

with m and q , the particle mass and electric charge, respectively. The numerical particles followed in the simulations correspond to q_f physical particles, with

$$q_f = \frac{nV}{N_{\text{pc}}} \quad (2.3)$$

with n the particle density, V the volume of a cell, and N_{pc} the number of numerical particles in a cell. A large enough number of particles is needed in order to obtain physical results. Indeed, an insufficient number of particles leads to numerical heating [11]. Usually, a minimum of 100 particles per cell is used, but recent results seem to encourage to use more particles [12].

2.1.2 The Monte Carlo collisions

In PIC simulations, collisions between charged and neutral particles can be modeled by binary collision, but this approach is computationally costly. Instead, a Monte-Carlo algorithm can be used [13]. This approach is very efficient and allows scattering, momentum transfer, and ionization to be consistently modeled. The propellant used in Hall Effect Thruster (HET) is xenon (Xe). The cross-sections used for modeling Xe or other gases collisions are taken from the LXCAT database project [14, 15]. Unless otherwise stated, the elastic, inelastic scattering and ionization reactions listed in Table 2.1 are used. The cross-section values are summarized in Fig. 2.1.

In the context of this thesis, and except precised otherwise, the ‘PIC simulation’ refers to the ‘PIC-Monte Carlo Collision (MCC) simulation’. In the case where no collision is modeled, we also call it ‘collisionless simulation’.

TABLE 2.1 – Reactions for xenon used in the PIC simulations

Reaction	Threshold	Reference
<i>Elastic scattering</i>		
$e + \text{Xe} = e + \text{Xe}$	–	[1, 2]
<i>Excitation</i>		
$e + \text{Xe} = e + \text{Xe}^*$	8.315eV	[1, 2]
$e + \text{Xe} = e + \text{Xe}^*$	9.447eV	[1, 2]
$e + \text{Xe} = e + \text{Xe}^*$	9.917eV	[1, 2]
$e + \text{Xe} = e + \text{Xe}^*$	11.7eV	[1, 2]
<i>Ionization</i>		
$e + \text{Xe} = e + \text{Xe}^+$	12.13eV	[1, 2]

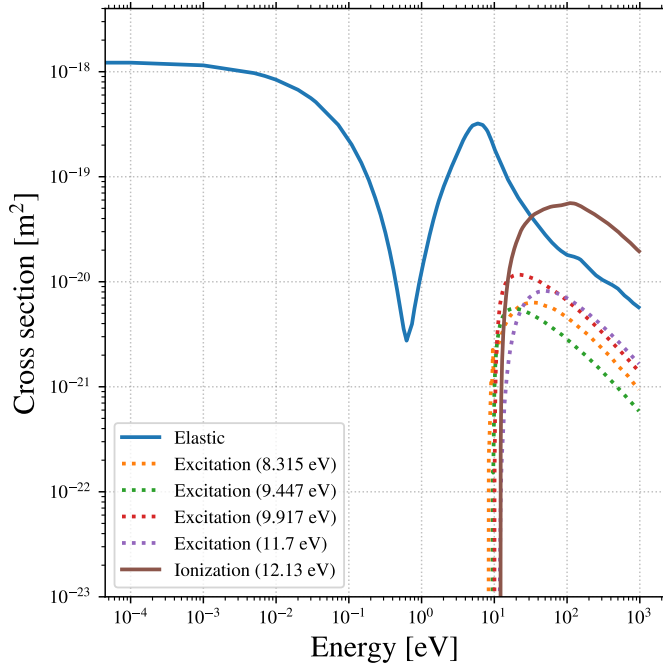


FIGURE 2.1 – Cross section values used in the Monte Carlo procedure [1, 2].

Chapitre 3

Impact of the dielectric walls on the anomalous electron mobility

Part of the work presented in this chapter has been published in Tavant et al. [16].

Lorem ipsum dolor sit amet, consectetur adipiscing elit. Ut purus elit, vestibulum ut, placerat ac, adipiscing vitae, felis. Curabitur dictum gravida mauris. Nam arcu libero, nonummy eget, consectetur id, vulputate a, magna. Donec vehicula augue eu neque. Pellentesque habitant morbi tristique senectus et netus et malesuada fames ac turpis egestas. Mauris ut leo. Cras viverra metus rhoncus sem. Nulla et lectus vestibulum urna fringilla ultrices. Phasellus eu tellus sit amet tortor gravida placerat. Integer sapien est, iaculis in, pretium quis, viverra ac, nunc. Praesent eget sem vel leo ultrices bibendum. Aenean faucibus. Morbi dolor nulla, malesuada eu, pulvinar at, mollis ac, nulla. Curabitur auctor semper nulla. Donec varius orci eget risus. Duis nibh mi, congue eu, accumsan eleifend, sagittis quis, diam. Duis eget orci sit amet orci dignissim rutrum.

Nam dui ligula, fringilla a, euismod sodales, sollicitudin vel, wisi. Morbi auctor lorem non justo. Nam lacus libero, pretium at, lobortis vitae, ultricies et, tellus. Donec aliquet, tortor sed accumsan bibendum, erat ligula aliquet magna, vitae ornare odio metus a mi. Morbi ac orci et nisl hendrerit mollis. Suspendisse ut massa. Cras nec ante. Pellentesque a nulla. Cum sociis natoque penatibus et magnis dis parturient montes, nascetur ridiculus mus. Aliquam tincidunt urna. Nulla ullamcorper vestibulum turpis. Pellentesque cursus luctus mauris.

Contents

3.1	Presentation of the study	12
3.2	The base case	14
3.2.1	Initial phase of the simulation : $t < 2 \mu\text{s}$	14
3.2.2	Saturated quasi steady-state : $t \geq 2 \mu\text{s}$	15
3.2.3	Enhanced electron transport	16

3.1 Presentation of the study

As introduced in Chapter 2, the Hall Effect Thruster (HET) behavior depends strongly on the axial electron transport toward the anode across the magnetic barrier. Two main phenomena are proposed to enhance the electron mobility,

- plasma instabilities and in particular the azimuthal Electron Cyclotron Drift Instability (ECDI), extensively studied in ??
- the electron induced electron emission from the wall

In order to compare quantitatively the relative importance of the two phenomena, we propose to conduct a parametric study on the dielectric wall characteristics. As highlighted in the introduction and in ??, the ECDI rises due to the $E \times B$ electron drift, but saturates due to both the axial convection which limits the electron heating, and the ion-wave trapping.

The first section describes the parameters of the simulation, while the second section highlights the main characteristics of the base simulation results (electron mobility, plasma potential, electron mobility, etc.). The other sections of the chapter present the results of the parametric study on the wall characteristics: first we study in ?? the influence of the dielectric layer, then in ?? the secondary electron emission is analyze, and lastly we combine the two characteristics in ??.

more informations could be added here !

The simulation domain corresponds to the exit plane of the thruster. Hence, a neutral pressure P_n of 0.1 mTorr and a plasma density n_e of $1 \times 10^{17} \text{ m}^{-3}$ are used. The fixed axial electric field and radial magnetic field are $E_z = 2 \times 10^4 \text{ V/m}$ and $B_r = 200 \text{ G}$, respectively. The rectangular 2D domain measures $L_r = 2 \text{ cm}$ in the radial dimension and $L_\theta = 0.5 \text{ cm}$ in the azimuthal direction. The axial length used for the convection is set to $L_z = 1 \text{ cm}$. It is important to note that the results shown in this chapter have been obtained at the beginning of my thesis, before the study of the convection presented in Chapter 2. Hence, in this chapter we use the convection model of Lafleur et al. [17]. However, we have validated that the convection model used does not modify the results under the conditions studied. The numerical parameters are chosen to respect the stability criterion of Particle In Cell (PIC) simulation, and are presented in Table 3.1

The simulation is initialized with a uniform density of particles, following a Maxwellian distribution with temperatures $T_{e,0}$ and $T_{i,0}$ for the electrons and the ions, respectively.

unsure
here

TABLE 3.1 – Standard operating and numerical parameters used in the 2D PIC simulations of an HET. The simulation results are given as representative values.

Physical Parameter	notation	Value	Unit
Gas		Xenon	-
Domain dimensions	$L_x \times L_y \times L_z$	$2.0 \times 0.5 \times 1.0$	[cm ³]
Radial magnetic field	B_0	200	[G]
Axial electric field	E_0	2×10^4	[Vm ⁻¹]
Mean plasma density	n_0	3×10^{17}	[m ⁻³]
Initial electron temperature	$T_{e,0}$	10.0	[V]
Initial ion temperature	$T_{i,0}$	0.1	[V]
Secondary electron temperature	T_{see}	1.0	[V]
Neutral gas pressure	P_n	1.0	[mTorr]
Neutral gas temperature	T_n	300	[K]
Neutral gas density	n_g	3.22×10^{19}	[m ⁻³]
Simulation Parameter			
Time step	Δt	4×10^{-12}	[s]
Cell size	$\Delta x = \Delta y$	2×10^{-5}	[m]
Number of particles per cell	N/NG	80	[part/cell]
Typical quantities			
Electron plasma frequency	ω_{pe}	3.1×10^{10}	[rad/s]
Ion plasma frequency	ω_{pi}	36×10^6	[rad/s]
Electron cyclotron frequency	ω_{ce}	3.5×10^9	[rad/s]
Electron Larmor radius	r_{Le}	6×10^{-4}	[m]

3.2 The base case

The *base* case corresponds to the case when the walls are grounded, and are fully absorbing. It is the reference case that will be extensively described and commented. Then, it will be used as reference to analyze and quantify the effects of two characteristics of the dielectric walls on the studied discharges : the secondary electron emission, and the modification of the electrostatic boundary condition.

3.2.1 Initial phase of the simulation: $t < 2 \mu\text{s}$

The initial phase of the simulation corresponds to the growth of the ECDI, and the formation of the sheaths. Because of the growth of the instability, the electron transport increases as well, which increases the electron heating. The time scale of the sheath formation is governed by the ion inertia. It is roughly the same time scale as the saturation of the instability due to ion-trapping.

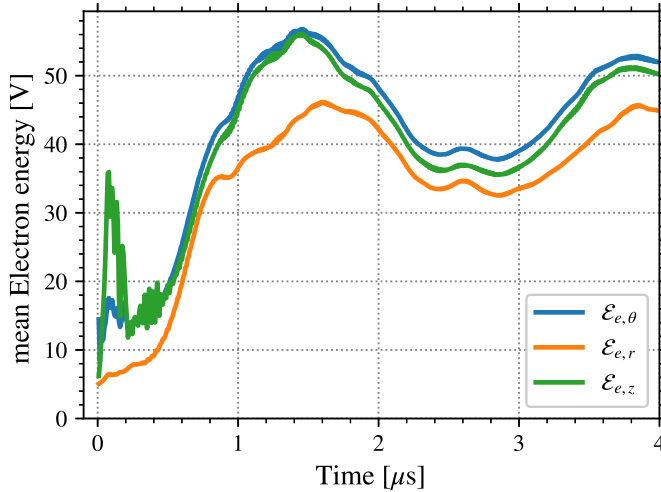


FIGURE 3.1 – Temporal evolution of the electron mean kinetic energy decomposed over the three directions. Only the beginning of the simulation is shown.

Figure 3.1 shows the temporal evolution of the electron mean kinetic energy decomposed over the three directions, $\mathcal{E}_{er}, \mathcal{E}_{e\theta}, \mathcal{E}_{ez}$, such that

$$\mathcal{E}_{ed} = \frac{1}{n} \frac{1}{2} m_e \iiint_{\mathbf{v}} v_{e,d}^2 f(\mathbf{v}) d^3v, \text{ with } d \in \{r, \theta, z\} \quad (3.1)$$

The mean kinetic energy is the sum of the thermal energy and the kinetic energy of the mean velocity. Because the electrons drift mainly in the azimuthal direction,

we have

$$\begin{cases} \mathcal{E}_{er} \simeq \frac{T_{er}}{2} \\ \mathcal{E}_{ez} \simeq \frac{T_{ez}}{2} \\ \mathcal{E}_{e\theta} \simeq \frac{T_{e\theta}}{2} + \frac{m_e}{2} \left(\frac{E_0}{B_0} \right)^2 \end{cases} \quad (3.2)$$

with $\frac{m_e}{2} \left(\frac{E_0}{B_0} \right)^2 \simeq 2.84 \text{ V}$. We see that after some high frequency oscillations of $\mathcal{E}_{e\theta}$ and \mathcal{E}_{ez} due to the cyclotron motion, the energies rise before stabilizing at $\mathcal{E}_e \simeq 45 \text{ V}$. The radial kinetic energy \mathcal{E}_{er} is less than \mathcal{E}_{ez} and $\mathcal{E}_{e\theta}$, but only by a small difference of 5 V, corresponding to roughly 10%. The small difference between the azimuthal and the axial kinetic energy is of the order of 2 V, as expected from the cyclotron motion of the electrons and Eq. (3.2). This means that the electrons are almost isotropic.

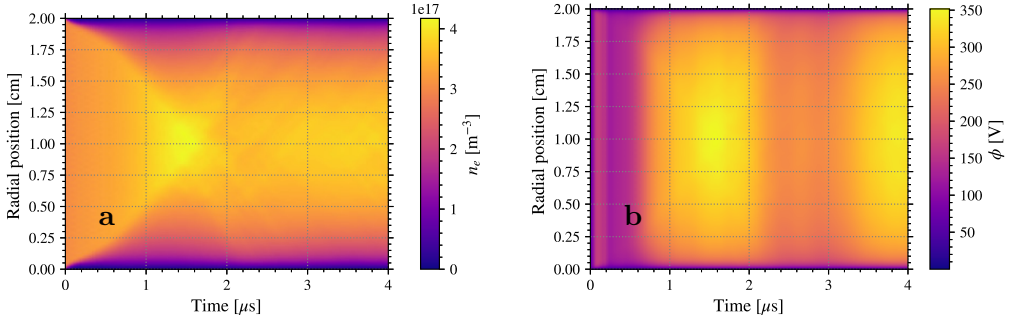


FIGURE 3.2 – Temporal evolution of the radial profile of the (a) electron density and (b) the plasma potential averaged azimuthally.

We can see in Figure 3.2 the evolution of the radial profile of the electron density on the plasma potential over the same period as Fig. 3.1. We observe on both quantities the formation of the sheath and the evolution toward a steady-state.

3.2.2 Saturated quasi steady-state: $t \geq 2 \mu\text{s}$

After the relatively fast rise of the plasma characteristics, the simulation reaches a quasi steady-state, as we can see in Figure 3.3. We observe that after $t \simeq 2 \mu\text{s}$, the electron energy \mathcal{E}_e starts to oscillate around a mean value. The oscillations are then damped and reach their minimum amplitude at $t \simeq 7 \mu\text{s}$ and then remain with a small amplitude as shown on simulations carried out up to $25 \mu\text{s}$ in Fig. 3.3 (the origin of these oscillations has been discussed in ??).

Figure 3.4 shows the azimuthally-averaged radial profiles of the electron and ion densities. The plasma is mostly quasineutral, except close to the walls, in the sheath, where the electron density falls more rapidly compared to that of ions. The sheath length can be roughly estimated to be 1 mm. The Debye length in our

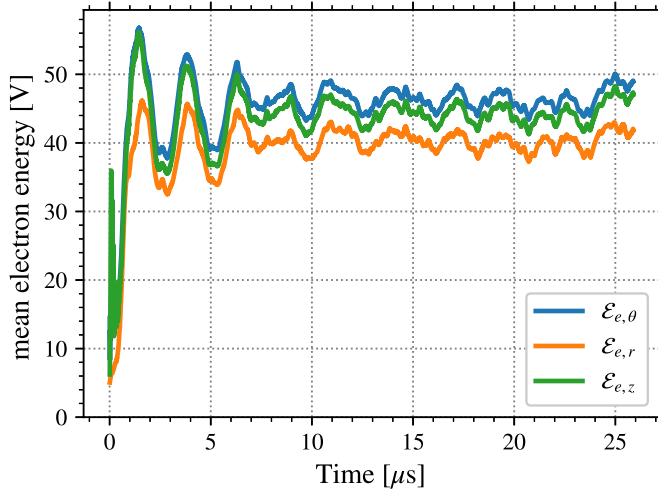


FIGURE 3.3 – Temporal evolution of the electron mean kinetic energy decomposed over the three directions, similar to Fig. 3.1 but for a longer period. We still see the difference between \mathcal{E}_{ez} and $\mathcal{E}_{e\theta}$ due to the $E \times B$ drift, and the colder radial energy.

conditions is

$$\lambda_D = \sqrt{\frac{\epsilon_0 k_b T_e}{n_e e^2}} \sim 0.4 \text{ mm}, \quad (3.3)$$

which corresponds to the expected floating sheath length [18] (a few λ_{De}).

3.2.3 Enhanced electron transport

As introduced in ??, the electron cross-field axial transport is characterized by the electron mobility

$$\mu_e = \frac{u_{e,z}}{E_z} \quad (3.4)$$

with $u_{e,z}$ and E_z the electron mean axial velocity and the axial electric field, respectively. In PIC simulations, μ_e is computed at each time step by

$$\mu_{\text{PIC}} = \frac{1}{NE_z} \sum_N v_{e,z} \quad (3.5)$$

Figure 3.5 shows the temporal evolution of the electron mobility μ_{PIC} measured in the simulation with Eq. (3.5). We can see that it presents the same characteristics as the evolution of the electron energy \mathcal{E}_e on Fig. 3.3. We recall that the classical electron mobility from the collisional theory developed in ?? is [17]

$$\mu_{\text{classical}} = \frac{\nu_m \frac{e}{m_e}}{\omega_{ce}^2 + \nu_m^2} \quad (3.6)$$

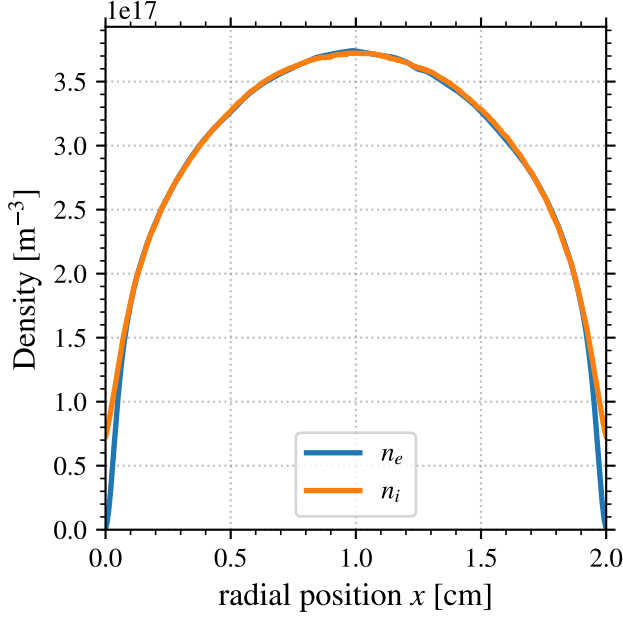


FIGURE 3.4 – Radial profile of the ion and electron densities at steady-state, averaged azimuthally and in time over the 5 last microseconds.

with ν_m the electron-neutral collision frequency and ω_{ce} is the electron cyclotron frequency. In the conditions of Table 3.1, $\mu_{\text{classical}} \simeq 0.8 \text{ m}^2(\text{sV})^{-1}$.

The measured electron mobility in the PIC simulation is one order of magnitude larger than the classical mobility. In the present case, as no electron is emitted from the wall, the enhancement can only come from the instabilities present in the plasma.

The oscillations can be seen in ??, which shows the azimuthal electric field observed at $T = 4 \mu\text{s}$. It clearly features the oscillation of wavelength of the order of 1 mm, as observed in Héron and Adam [19], and Janhunen et al. [12]. Figure 3.6 shows the temporal evolution of the azimuthal electric field measured at the center of the channel. We can see that the instability rises and saturates quickly. Then, the oscillation remains quite stable. The Fourier Transform of the electric field presents a clear maximum at 14 MHz. The theoretical frequency of the ECDI instability is [20]

$$f_{\text{max}} = \frac{\omega_{pi}}{\sqrt{3}} \simeq 21 \text{ MHz}, \quad (3.7)$$

which gives a relatively good agreement with the oscillation observed. The ECDI instability was the subject of ??, hence it will not be further discussed here.

The effective mobility μ_{eff} is determined by the correlation term $\langle \delta E_\theta \delta n_e \rangle$ and the parameters of the simulations. The effective mobility at saturation $\mu_{\text{eff}}^{\text{sat}}$,

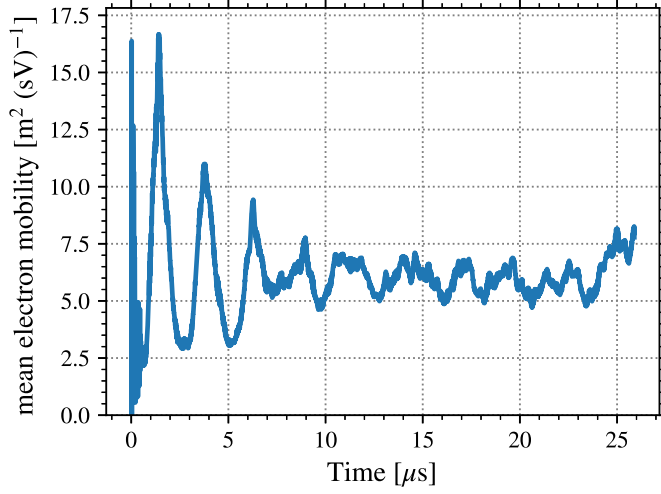


FIGURE 3.5 – Temporal evolution of the electron axial mobility computed in the PIC simulation.

using the hypothesis of saturation by ion-wave trapping, only needs the electron temperature T_e . We can see that the three values μ_{PIC} , μ_{eff} , and $\mu_{\text{eff}}^{\text{sat}}$ are close from each-others.

TABLE 3.2 – Characteristics measured in the simulation at $t = 27 \mu\text{s}$.

Quantity	Value
Correlation $\langle \delta E_\theta \delta n_e \rangle$	$6 \times 10^{20} \text{ V/m}^4$
Effective mobility μ_{eff} from ??	$4.4 \text{ m}^2(\text{sV})^{-1}$
Mobility saturation $\mu_{\text{eff}}^{\text{sat}}$ from ??	$3.3 \text{ m}^2(\text{sV})^{-1}$
Measured mobility μ_{PIC} from Eq. (3.5)	$6 \text{ m}^2(\text{sV})^{-1}$

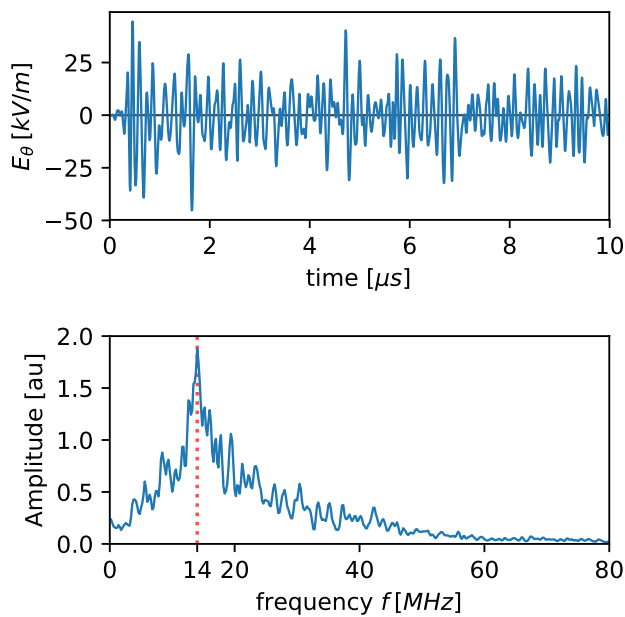


FIGURE 3.6 – Azimuthal instability: temporal evolution of the azimuthal electric field at the center of the simulations, and its frequency spectrum computed by FFT. The frequency for which the amplitude is maximum is highlighted.

Chapitre 4

Conclusion

4.1 Summary of the thesis

Lorem ipsum dolor sit amet, consectetur adipiscing elit. Ut purus elit, vestibulum ut, placerat ac, adipiscing vitae, felis. Curabitur dictum gravida mauris. Nam arcu libero, nonummy eget, consectetur id, vulputate a, magna. Donec vehicula augue eu neque. Pellentesque habitant morbi tristique senectus et netus et malesuada fames ac turpis egestas. Mauris ut leo. Cras viverra metus rhoncus sem. Nulla et lectus vestibulum urna fringilla ultrices. Phasellus eu tellus sit amet tortor gravida placerat. Integer sapien est, iaculis in, pretium quis, viverra ac, nunc. Praesent eget sem vel leo ultrices bibendum. Aenean faucibus. Morbi dolor nulla, malesuada eu, pulvinar at, mollis ac, nulla. Curabitur auctor semper nulla. Donec varius orci eget risus. Duis nibh mi, congue eu, accumsan eleifend, sagittis quis, diam. Duis eget orci sit amet orci dignissim rutrum.

Nam dui ligula, fringilla a, euismod sodales, sollicitudin vel, wisi. Morbi auctor lorem non justo. Nam lacus libero, pretium at, lobortis vitae, ultricies et, tellus. Donec aliquet, tortor sed accumsan bibendum, erat ligula aliquet magna, vitae ornare odio metus a mi. Morbi ac orci et nisl hendrerit mollis. Suspendisse ut massa. Cras nec ante. Pellentesque a nulla. Cum sociis natoque penatibus et magnis dis parturient montes, nascetur ridiculus mus. Aliquam tincidunt urna. Nulla ullamcorper vestibulum turpis. Pellentesque cursus luctus mauris.

4.1.1 Growth and saturation of the azimuthal instability

Lorem ipsum dolor sit amet, consectetur adipiscing elit. Ut purus elit, vestibulum ut, placerat ac, adipiscing vitae, felis. Curabitur dictum gravida mauris. Nam arcu libero, nonummy eget, consectetur id, vulputate a, magna. Donec vehicula augue eu neque. Pellentesque habitant morbi tristique senectus et netus et malesuada fames ac turpis egestas. Mauris ut leo. Cras viverra metus rhoncus sem. Nulla et lectus vestibulum urna fringilla ultrices. Phasellus eu tellus sit amet tortor gravida placerat. Integer sapien est, iaculis in, pretium quis, viverra ac, nunc. Praesent eget sem vel leo ultrices bibendum. Aenean faucibus. Morbi dolor nulla, malesuada eu, pulvinar at, mollis ac, nulla. Curabitur auctor semper nulla. Donec varius orci eget risus. Duis nibh mi, congue eu, accumsan eleifend, sagittis quis, diam. Duis eget orci sit amet orci dignissim rutrum.

Nam dui ligula, fringilla a, euismod sodales, sollicitudin vel, wisi. Morbi auctor lorem non justo. Nam lacus libero, pretium at, lobortis vitae, ultricies et, tellus. Donec aliquet, tortor sed accumsan bibendum, erat ligula aliquet magna, vitae ornare odio metus a mi. Morbi ac orci et nisl hendrerit mollis. Suspendisse ut massa. Cras nec ante. Pellentesque a nulla. Cum sociis natoque penatibus et magnis dis parturient montes, nascetur ridiculus mus. Aliquam tincidunt urna. Nulla ullamcorper vestibulum turpis. Pellentesque cursus luctus mauris.

4.1.2 Impact of the wall characteristics on the plasma-wall interaction

Lorem ipsum dolor sit amet, consectetur adipiscing elit. Ut purus elit, vestibulum ut, placerat ac, adipiscing vitae, felis. Curabitur dictum gravida mauris. Nam arcu libero, nonummy eget, consectetur id, vulputate a, magna. Donec vehicula augue eu neque. Pellentesque habitant morbi tristique senectus et netus et malesuada fames ac turpis egestas. Mauris ut leo. Cras viverra metus rhoncus sem. Nulla et lectus vestibulum urna fringilla ultrices. Phasellus eu tellus sit amet tortor gravida placerat. Integer sapien est, iaculis in, pretium quis, viverra ac, nunc. Praesent eget sem vel leo ultrices bibendum. Aenean faucibus. Morbi dolor nulla, malesuada eu, pulvinar at, mollis ac, nulla. Curabitur auctor semper nulla. Donec varius orci eget risus. Duis nibh mi, congue eu, accumsan eleifend, sagittis quis, diam. Duis eget orci sit amet orci dignissim rutrum.

Nam dui ligula, fringilla a, euismod sodales, sollicitudin vel, wisi. Morbi auctor lorem non justo. Nam lacus libero, pretium at, lobortis vitae, ultricies et, tellus. Donec aliquet, tortor sed accumsan bibendum, erat ligula aliquet magna, vitae ornare odio metus a mi. Morbi ac orci et nisl hendrerit mollis. Suspendisse ut massa. Cras nec ante. Pellentesque a nulla. Cum sociis natoque penatibus et magnis dis parturient montes, nascetur ridiculus mus. Aliquam tincidunt urna. Nulla ullamcorper vestibulum turpis. Pellentesque cursus luctus mauris.

Annexe A

Scalability tests

In this annexe, we give more information on the scalability tests conducted. We conducted both a weak and a strong scalability tests. We recall that the strong scalability keeps the load constant while increasing the computational performance, here the number of CPU. The weak scalability keeps the load to the number of CPU ratio constant. However, it does not correspond to the need we had, which is to find the optimal number of CPU for a given task. Beside, the results of the weak scalability were less clear to analyze. Hence, we discarded them.

The parameters of the strong scalability test used are given in Table A.1. They are close to the parameter used in production, presented in Table 3.1. The smaller test-case uses the same settings, except for the domain which is divided by a factor of 4. The dielectric boundary conditions are not modeled (no Secondary Electron Emission (SEE), no dielectric layer). The Inputs, set-up, and Outputs are not taken into account in the study of the performances. However, the usual diagnostics (mean density, fluxes, temperature, at boundaries and in the plasma) are computed. The performances are averaged over the 1000 first time steps of the simulations. Hence, the load is well balanced between the CPU.

An example of the relative importance of each module of the simulation over a time step is given in Table A.3. Each module is called 1000 times, except for the outputs function, that writes the diagnostics to the disk, which is called only once. Its duration is divided by the number of time steps, in order to compare it to the other modules. To give an order of magnitude, taking $t = 10.08 \text{ s}$ for one time-step corresponds to an average of 8.2 ns per particle.

TABLE A.1 – Operating and numerical parameters used in the strong scalability large test-case.

Physical Parameter	notation	Value	Unit
Gas		Xenon	-
Domain dimensions	$L_x \times L_y$	1.0×1.023	[cm ²]
Radial magnetic field	B_0	200	[G]
Axial electric field	E_0	2×10^4	[Vm ⁻¹]
Mean plasma density	n_0	1×10^{17}	[m ⁻³]
Initial electron temperature	$T_{e,0}$	1.0	[V]
Initial ion temperature	$T_{i,0}$	0.05	[V]
Neutral gas pressure	P_n	0.1	[mTorr]
Neutral gas temperature	T_n	300	[K]
Neutral gas density	n_g	3.22×10^{18}	[m ⁻³]
Simulation Parameter			
Time step	Δt	4×10^{-13}	[s]
Cell size	$\Delta x = \Delta y = \Delta z$	5×10^{-7}	[m]
Number of particles per cell	N/NG	150	[part/cell]
Number of particles	N	2×614099924	[particles]
Number of time steps	N_t	1000	–

TABLE A.2 – Modified parameter for the strong-scalability small test-case. The other parameters are given in Table A.1.

Physical Parameter	notation	Value	Unit
Domain dimensions	$L_x \times L_y$	1.0×1.023	[cm ²]
Simulation Parameter			
Cell size	$\Delta x = \Delta y = \Delta z$	1×10^{-6}	[m]

TABLE A.3 – Performances of the large test-case (parameters of Table A.1) when using 96 CPUs, average over 1000 time steps.

Module	Duration one time-step [s]	Percentage
Total	10.08	100
Diagnostics particle to mesh	6.03	59.9
Particle motion	2.88	28.6
Monte Carlo Collision	0.729	7.31
Outputs	0.287	2.84
Poisson solver	0.075	0.75

Bibliography

- [1] A. Phelps. Phelps database. www.lxcat.net, retrieved on November 16 2016.
- [2] Cross sections extracted program MAGBOLTZ. www.lxcat.net, version 7.1 june 2016.
- [3] C. Boniface, J. Charbonnier, L. Lefebvre, V. Leroi, and T. Lienart. An Overview of electric propulsion activities at CNES. In *IEPC*, Georgia Institute of Technology, Atlanta, Georgia, USA, 2017.
- [4] O. Duchemin, J. Rabin, L. Balika, M. Diome, J.-M. Lonchard, and X. Cavelan. Development Status of the PPS@5000 Hall Thruster Unit. In *IEPC-2017-415*, Georgia Institute of Technology, Atlanta, Georgia, USA, 2017.
- [5] J. Vaudolon, V. Vial, N. Cornu, and I. Habbassi. PPS-X00 Hall Thruster Development at Safran. In *IAC*, Bremen, Germany, 2018.
- [6] C. Charles. Plasmas for spacecraft propulsion, *Journal of Physics D: Applied Physics*, 42(16):163001, 2009.
- [7] S. Mazouffre. Electric propulsion for satellites and spacecraft : Established technologies and novel approaches, *Plasma Sources Science and Technology*, 25(3):033002, 2016.
- [8] D. Lev, R. M. Myers, K. M. Lemmer, J. Kolbeck, H. Koizumi, and K. Polzin. The technological and commercial expansion of electric propulsion, *Acta Astronautica*, 2019.
- [9] S. Samukawa, M. Hori, S. Rauf, K. Tachibana, P. Bruggeman, G. Kroesen, J. C. Whitehead, A. B. Murphy, A. F. Gutsol, S. Starikovskaia, U. Kortshagen, J.-P. Boeuf, T. J. Sommerer, M. J. Kushner, U. Czarnetzki, and N. Mason. The 2012 Plasma Roadmap, *Journal of Physics D: Applied Physics*, 45(25):253001, 2012.
- [10] P. Lascombes. Electric Propulsion For Small Satellites Orbit Control And Deorbiting : The Example Of A Hall Effect Thruster. In *15th International*

- Conference on Space Operations*, Marseille, France, 2018. American Institute of Aeronautics and Astronautics.
- [11] H. Ueda, Y. Omura, H. Matsumoto, and T. Okuzawa. A study of the numerical heating in electrostatic particle simulations *Computer physics communications*, 79(2) :249–259, 1994.
 - [12] S. Janhunen, A. Smolyakov, D. Sydorenko, M. Jimenez, I. Kaganovich, and Y. Raitses. Evolution of the electron cyclotron drift instability in two-dimensions, *Physics of Plasmas*, 25(8):082308, 2018.
 - [13] V. Vahedi, M. A. Lieberman, G. DiPeso, T. D. Rognlien, and D. Hewett. Analytic model of power deposition in inductively coupled plasma sources, *Journal of Applied Physics*, 78(3):1446–1458, 1995.
 - [14] LXCat project. www.lxcat.net, 2019.
 - [15] S. Pancheshnyi, S. Biagi, M. Bordage, G. Hagelaar, W. Morgan, A. Phelps, and L. Pitchford. The LXCat project : Electron scattering cross sections and swarm parameters for low temperature plasma modeling, *Chemical Physics*, 398:148–153, 2012.
 - [16] A. Tavant, V. Croes, R. Lucken, T. Lafleur, A. Bourdon, and P. Chabert. The effects of secondary electron emission on plasma sheath characteristics and electron transport in an E x B discharge via kinetic simulations, *Plasma Sources Science and Technology*, 27(12):124001, 2018.
 - [17] T. Lafleur, S. D. Baalrud, and P. Chabert. Theory for the anomalous electron transport in Hall effect thrusters. I. Insights from particle-in-cell simulations, *Physics of Plasmas*, 23(5):053502, 2016.
 - [18] P. Chabert. What is the size of a floating sheath?, *Plasma Sources Science and Technology*, 23(6):065042, 2014.
 - [19] A. Héron and J. C. Adam. Anomalous conductivity in Hall thrusters : Effects of the non-linear coupling of the electron-cyclotron drift instability with secondary electron emission of the walls *Physics of Plasmas*, 20(8) :082313, 2013.
 - [20] T. Lafleur, S. D. Baalrud, and P. Chabert. Characteristics and transport effects of the electron drift instability in Hall-effect thrusters, *Plasma Sources Science and Technology*, 26(2):024008, 2017.

Titre: Titre de la thèse

Mots clés: mots clés

Résumé:

Lorem ipsum dolor sit amet, consectetur adipiscing elit. Ut purus elit, vestibulum ut, placerat ac, adipiscing vitae, felis. Curabitur dictum gravida mauris. Nam arcu libero, nonummy eget, consectetur id, vulputate a, magna. Donec vehicula augue eu neque. Pellentesque habitant morbi tristique senectus et netus et malesuada fames ac turpis egestas. Mauris ut leo. Cras viverra metus rhoncus sem. Nulla et lectus vestibulum urna fringilla ultrices. Phasellus eu tellus sit amet tortor gravida placerat. Integer sapien est, iaculis in, pretium quis, viverra ac, nunc. Praesent eget sem vel leo ultrices bibendum. Aenean faucibus. Morbi dolor nulla, malesuada eu, pulvinar at, mollis ac, nulla. Cu-

rabitur auctor semper nulla. Donec varius orci eget risus. Duis nibh mi, congue eu, accumsan eleifend, sagittis quis, diam. Duis eget orci sit amet orci dignissim rutrum.

Nam dui ligula, fringilla a, euismod sodales, sollicitudin vel, wisi. Morbi auctor lorem non justo. Nam lacus libero, pretium at, lobortis vitae, ultricies et, tellus. Donec aliquet, tortor sed accumsan bibendum, erat ligula aliquet magna, vitae ornare odio metus a mi. Morbi ac orci et nisl hendrerit mollis. Suspendisse ut massa. Cras nec ante. Pellentesque a nulla. Cum sociis natoque penatibus et magnis dis parturient montes, nascetur ridiculus mus. Aliquam tincidunt urna. Nulla ullamcorper vestibulum turpis. Pellentesque cursus luctus mauris.

Title: Title

Keywords: keywords

Abstract: Lorem ipsum dolor sit amet, consectetur adipiscing elit. Ut purus elit, vestibulum ut, placerat ac, adipiscing vitae, felis. Curabitur dictum gravida mauris. Nam arcu libero, nonummy eget, consectetur id, vulputate a, magna. Donec vehicula augue eu neque. Pellentesque habitant morbi tristique senectus et netus et malesuada fames ac turpis egestas. Mauris ut leo. Cras viverra metus rhoncus sem. Nulla et lectus vestibulum urna fringilla ultrices. Phasellus eu tellus sit amet tortor gravida placerat. Integer sapien est, iaculis in, pretium quis, viverra ac, nunc. Praesent eget sem vel leo ultrices bibendum. Aenean faucibus. Morbi dolor nulla, malesuada eu, pulvinar at, mollis ac, nulla. Curabitur auctor semper

nulla. Donec varius orci eget risus. Duis nibh mi, congue eu, accumsan eleifend, sagittis quis, diam. Duis eget orci sit amet orci dignissim rutrum.

Nam dui ligula, fringilla a, euismod sodales, sollicitudin vel, wisi. Morbi auctor lorem non justo. Nam lacus libero, pretium at, lobortis vitae, ultricies et, tellus. Donec aliquet, tortor sed accumsan bibendum, erat ligula aliquet magna, vitae ornare odio metus a mi. Morbi ac orci et nisl hendrerit mollis. Suspendisse ut massa. Cras nec ante. Pellentesque a nulla. Cum sociis natoque penatibus et magnis dis parturient montes, nascetur ridiculus mus. Aliquam tincidunt urna. Nulla ullamcorper vestibulum turpis. Pellentesque cursus luctus mauris.



Titre : Étude numérique du transport des électrons dans un propulseur à effet Hall

Mots clés : Propulsion électrique, propulseur de Hall, simulation PIC, benchmark, instabilités

Résumé : Ces dernières années, le nombre de satellites en orbite autour de la Terre a augmenté de manière exponentielle. Grâce à leur faible consommation en carburant, de plus en plus de propulseurs électriques sont utilisés à bord de ces satellites, notamment le propulseur de Hall qui est l'un des plus efficaces. De la diversité des applications découle le besoin d'avoir des propulseurs de taille et puissance variables. Cependant, la physique des propulseurs de Hall est encore méconnue et les nouveaux designs se font de manière empirique, avec un développement long et coûteux, pour un résultat final limité. Pour pallier ce problème, des codes de simulation peuvent être utilisés mais une meilleure compréhension des phénomènes clés est alors nécessaire, plus particulièrement du transport anormal des électrons qui doit être pris en compte de manière auto-consistante pour pouvoir capturer totalement le comportement de la décharge.

Ce transport étant relié à l'instabilité azimuthale de dérive électronique, un code 2D particulaire existant a été amélioré pour pouvoir simuler cette direction azimuthale mais aussi la direction axiale. Avant d'analyser le comportement de la décharge, ce code a été vérifié sur un cas de benchmark, avec 6 autres

codes particuliers développés par différents groupes de recherches internationaux. Ce cas simplifié a été ensuite utilisé pour vérifier de manière intensive un développement analytique pour estimer la force de friction électron-ion, qui est le témoin de la contribution des instabilités azimuthales sur le transport anormal. Puis, la dynamique des neutres a été rajoutée pour capturer de manière auto-consistante le comportement de la décharge. Une technique artificielle de loi d'échelle a été adoptée, avec une augmentation de la permittivité du vide, pour alléger les contraintes de stabilité du code particulaire et accélérer les simulations. Grâce à une parallélisation du code efficace, ce facteur artificiel a été réduit de manière significative, se rapprochant ainsi d'un cas proche de la réalité. La force de friction électron-ion a été observée comme étant celle qui contribuait le plus au transport anormal durant les oscillations basse-fréquence du mode de respiration. Pour finir, l'interaction complexe entre le mode de respiration, l'instabilité de transit des ions et l'instabilité de dérive électronique a aussi été étudiée, avec la formation de structures azimuthales à grande longueur d'onde, associées à un plus grand transport anormal.

Title : Numerical study of electron transport in Hall Thrusters

Keywords : Electric propulsion, Hall thruster, PIC simulation, benchmark, instabilities

Abstract : In the last decade, the number of satellites orbiting around Earth has grown exponentially. Thanks to their low propellant consumption, more and more electric thrusters are now used aboard these satellites, with the Hall thrusters being one of the most efficient. From the diversity of applications stems the need of widening the thruster power capabilities. However, due to a lack of knowledge on Hall thruster physics, this scaling is currently done empirically, which limits the efficiency of the newly developed thrusters and increases the development time and cost. To overcome this issue, numerical models can be used but a deeper understanding on key phenomena is still needed, more specifically on the electron anomalous transport which should be self-consistently accounted for to properly capture the discharge behaviour.

As this transport is related to the azimuthal electron drift instability, an existing 2D Particle-In-Cell code was further developed to simulate this azimuthal direction along with the axial direction in which the ions are accelerated, producing the thrust. Prior to analyse the discharge behaviour, this code has been verified

on a benchmark case, with 6 other PIC codes developed in different international research groups. This simplified case was later used to stress-test previous analytical developments to approximate the instability-enhanced electron-ion friction force which represents the contribution of the azimuthal instabilities to the anomalous transport. Then, the neutral dynamics has been included to capture the full self-consistent behaviour of the discharge. We used an artificial scaling technique, increasing the vacuum permittivity, to relax the PIC stability constraints and speed-up the simulations. Thanks to an efficient code parallelisation, we managed to reduce this scaling factor to a small value, hence simulating a case close to reality. The electron-ion friction force was found to be the main contributor to the anomalous transport throughout the whole low-frequency breathing mode oscillations. Finally, the complex interaction between the breathing mode, the ion-transit time instabilities and the azimuthal electron drift instabilities has been studied, with the formation of long-wavelength structures associated with an enhanced anomalous transport.

